CONF-800617--4

CHAR GASIFICATION AND ASH VAPORIZATION IN SINGLE-STAGE AND TWO-STAGE COAL-FIRED MHD COMBUSTORS

MASTER

T.W. Hastings and A.F. Sarofim
Department of Chemical Engineering
Massachusetts Institute of Technology
Cambridge, Massachusetts

Abstract

A computer model is presented for the simulation of coal combustion under conditions pertinent to single-stage and two-stage open-cycle MHD systems. The vaporization of mineral constituents is described by an external-diffusion controlled model, using empirical data for the effective vapor pressures. Chemical kinetics are included for the reactions of char with O_2, CO_2, H_2O, O, and OH. A parametric study of the effects of pressure, fuel/air equivalence ratio, and oxidant preheat temperature is used to illustrate tradeoffs between coal combustion efficiency, ash vaporization, and combustor residence time.

I. Introduction

It has become increasingly important to be able to estimate and regulate the amount of ash carried over from coal combustors in open-cycle MHD power plants, both in order to control the slag thickness in the MHD channel and to minimize slag-seed interaction. At the temperatures of interest for MHD a significant fraction of the ash may vaporize and this provides a lower limit on the amount of ash that will be carried over from the combustor to the channel and downstream components. The amount of ash vaporized will depend upon a number of design and operating variables, including air preheat, residence time, combustor pressure, fuel/air ratio, and oxygen enrichment. This paper provides a systematic evaluation of how these factors influence ash vaporization.

The paper incorporates the results of previous experimental studies on devolatilization, ash vaporization, and char combustion[1] into a computer model for simulating coal combustion under MHD conditions. The next two sections discuss the kinetics of char combustion and ash vaporization. The last sections illustrate the tradeoffs between carbon combustion efficiency and ash vaporization, which were studied parametrically by varying the pressure, fuel-to-oxidant equivalence ratio, and oxidant preheat temperature.

II. Char Gasification Kinetics for Single Particles

A detailed kinetic model has been developed to describe the instantaneous steady-state reaction rate of a burning char particle, including the reactions of carbon with CO_2, H_2O, O_2, O and OH, and making allowance for the effects of external boundary layer diffusion and internal pore diffusion. At the high temperatures encountered in MHD systems, the gas species external to the boundary layers of the burning particles can be considered to be in equilibrium. The reaction rate for each reactant is given by:

$$-\frac{1}{S_{EX}}\frac{dN_i}{dt} = C_{ig}\Big/\left(\left(\frac{T_{BL}}{T_g}\right)\frac{1}{K_i} + \left(\frac{T_p}{T_g}\right)\frac{S_{EX}/V_p}{k_i\,(\xi_i f_{IN} + f_{EX})}\right) \qquad (1)$$

where the first term in the denominator represents the boundary layer resistance and the second the reaction on internal and external surfaces (see nomenclature). The effectiveness factor given in Reference (2) for spherical particles was used, taking into account both molecular and Knudsen diffusion within the pores[3,4]. The molar rate of char consumption for reaction i can be obtained from Equation (1) from the following molar balance:

$$R_i = \frac{\alpha_i}{S_{EX}}\frac{dN_i}{dt} \qquad (2)$$

An energy balance for the particle can also be written to include the enthalpy of reaction, convection, and radiation to both the combustor wall and to the gas:

$$\sum_{i=1}^{5}[R_i(-\Delta H_{RX,i})] = h(T_p - T_g) + (1-\varepsilon_g)\sigma(T_p^4 - T_W^4) + \varepsilon_g\sigma(T_p^4 - T_g^4) \qquad (3)$$

A list of assumptions is given in Table 1.

Calculations were performed using an iterative solution by selecting parameters from the range of conditions shown in Table 2. The selection of rate parameters, which were extrapolated to high temperatures, was discussed previously[1]. Results for the effect of temperature and equivalence ratio are shown in Figures 1(a) and 1(b) for particle diameters of 10 and 150μm, encompassing the range of interest. The total reaction rate is seen to decrease rapidly as the equivalence ratio is increased beyond 2. The results in Figure 1 are for 1 atmosphere total pressure; slightly higher rates were calculated at 5 atmospheres pressure.

The fraction of the total rate due to each reaction is shown in Figures 2(a) and 2(b) for two values of ϕ_{EFF} for a 10μm particle. The reactions of the char with CO_2 and H_2O dominate for gas temperatures below 2100°K at $\phi_{EFF} = 1.1$, and their control extends to higher temperatures for $\phi = 2.4$ until the reactions with oxygen atoms and hydroxyl radicals become important. For particles larger than 10μm, the CO_2 and H_2O reactions are even more important due to increased utilization of the internal surface area relative to O_2, O and OH. These latter three exothermic reactions are essentially limited by external mass transport under most conditions.

The fraction of the rate attributable to each species is shown in Figures 3(a) and 3(b) as computed for a total pressure of 5 atmospheres. Increasing the total pressure results in a striking shift in the temperature range over which the CO_2 and H_2O are the dominant reactants, since these species are dissociated to a lesser extent than at 1 atmosphere.

As noted earlier, the gas compositions used in this analysis correspond to those existing in the later stages of char burnout in combustors operating at an overall fuel-rich stoichiometry for the

DISCLAIMER

Table 1: Assumptions for Single Particle Model.

- Spherical particle.
- Gas Phase at equilibrium.
- Gas is fuel-rich mixture of coal and air, specified by an effective fuel/air equivalence ratio.
- External diffusion properties calculated at average of gas and particle temperatures.
- Intrinsic reactions are first order kinetic processes.
- Pore structure properties assumed to be those of raw char sample.
- Pore structure does not change and is well characterized by a single average pore size and surface per unit weight for cylindrical pores.
- Particle is isothermal throughout.
- Steady state conditons exist.
- Transport properties are calulated by mixture relations using concentrations of each species in bulk gas, both for properties inside pores and in external diffusion film.
- Assumed parameters for energy balance included $\epsilon_g = 0.3$ and specification of wall temperature.
- Convective heat transfer coefficient described by Nusselt number of 2; mass transfer coefficient for each species described by Sherwood number of 2.

Table 2: Range of Parameters for Single Particle Study.

1500°K	≤	T_g	≤	3000°K
1 atm	≤	P	≤	5 atm
10 μm	≤	d_p	≤	150 μm
1.0	≤	ϕ_{EFF}	≤	2.4

coal/air feed. The trends indicated above show that the overall reaction rate depends critically on the local conditons at each point in the combustor. For two-stage systems with a fuel-rich first stage the reactions with CO_2 and H_2O are very important in obtaining a high degree of char burnout. This finding will be demonstrated more clearly in section IV, where the single particle model is used in a global combustor model for both single and two-stage combustors.

III. Ash Vaporization Kinetics

The rate of vaporization of the different mineral constituents is governed by the complex factors that determine their effective vapor pressures in the burning coal particles. The computation of vaporization rates is complicated by the fact that mineral constituents within a coal particle fuse and coalesce during combustion, and the composition of the multicomponent mixtures change with time. A further complication is that the vapor pressure of the constituents in the ash will depend upon the vapor pressure of species formed in the locally reducing conditions prevalent in the coal particle. The high vapor pressure of reduced species such as SiO and AlO contribute to a much higher vaporization rate than would be expected for the higher oxides. Prediction of the rate of ash vaporization from thermodynamic data is not possible at this stage and we have relied on experimental results obtained in a parallel study at M.I.T. The vaporization rates of individual constituents of a coal were measured over the temperature range of 1800 to 3000°K. The vaporization rates could be correlated empirically by assuming rate control by mass transfer from the particle, with the effective vapor pressure $P_i(T_g)$ at the particle surface obtained from the experimental results.[5]

The rate of change of the fraction F_i of species I in the original coal which has vaporized can be represented by:

$$\frac{dF_i}{dt} = \frac{3}{r_{po}^3 C_{io} R T_p} \cdot D_i(T_{BL}) \cdot r_p(t) \cdot P_i(T_p) \qquad (4)$$

where $r_p(t)$ is the particle radius at time t, r_{po} is the initial particle radius, and C_{io} is the initial molar concentration of species i in the particle. The temperature dependence of the vapor pressure is correlated by:

$$P_i(T_p) = A_i \exp\left[\frac{-B_i}{RT_p}\right] \qquad (5)$$

where A_i and B_i are empirical factors whose values are shown in Table 3 for Montana lignite coal. These values were obtained by integration of Equation (4) and regression of the experimental data. The values of A_i and B_i are expected to vary with coal type. Although restricted to the Montana lignite, the parameters listed in Table 3 should demonstrate the trends resulting from changes in operating conditions for any coal.

IV. Coal Combustor Model

A computer model has been assembled to simulate coal combustion in an aerodynamically simple MHD combustor for conditions pertinent to single and multi-stage units. This model furnishes a framework for incorporating available experimental data on various aspects of the combustion process and for testing the sensitivity to specific parameters.

Model Description

Values are selected for the coal flowrate, overall stoichiometry, combustor geometry, and operating conditions. The coal, composed of C, H, O, N, S and mineral matter components, is assumed to undergo an instantaneous devolatilization which liberates all of the H, O, N and S and a fraction of the initial carbon (70% in this study). The remaining char particles are asigned size number densities according to a Rosin-Rammler distribution, allowing for the density change due to swelling. Volatiles mix with the oxidant, whose composition and preheat temperature are specified. An initial equilibrium state is then calculated, corresponding to burning of the volatiles and heatup of the char particles.

The mixture then enters a plug flow reactor where the char particles burn in a pseudo-steady-state manner according to the single particle model described earlier. Reaction rates include internal burning contributions, but char particles are described by a shrinking sphere model with constant density and internal pore structure. Ash vaporization is calculated as an external diffusion controlled phenomena with allowance for thermal effects.

Table 3: Values of Constants A and B for Ash Vaporization Model for Montana Lignite		
Species	A(Atm)	(B/R) x 10^{-4}(°K)
Al_2O_3	2.32	2.93
As_2O_3	1.27 x 10^{-4}	1.55
CaO	.714	1.86
Fe_2O_3	.496	2.26
MgO	24.2	2.34
Na_2O	7.77 x 10^{-4}	1.29
SiO_2	7.67	2.60
ZnO	3.73 x 10^{-3}	2.04

Enthalpy and mass balances are calculated for each incremental plug flow section, considering wall heat loses to be due to particulate and banded gas radiation and convection. The gas phase species are assumed to be in chemical equilibrium, with vaporized ash constituents taken as inert species.

Single Stage

The results of a typical calculation for a single-stage combustor are presented in Figure 4, which shows the time dependence of coal burnout, gas temperature, and wall heat loss. The gas temperature initially rises rapidly, and levels off as the rate of char consumption decreases and as the total wall heat loss rises. For the same conditions, Figure 5(a) shows the contributions of the gaseous reactants to the total rate and 5(b) shows the composition of the ash vaporized, both reported as a function of the amount of coal burned. The reactions of the char residue with CO_2 and H_2O are found to be as important as the reaction with O_2, and a significant contribution from OH is also predicted.

The calculated effects of fuel/air equivalence ratio and residence time on coal burnout and ash vaporization are shown in Figure 6(a). In the fuel-lean case burnout is achieved more quickly than for either stoichiometric or fuel-rich conditions, but this is accompanied by a higher ash vaporization rate since higher temperatures are attained at the start of the combustion process. Figure 6(b) shows the effects of pressure and air preheat on coal burnout. For any given pressure, increasing the preheat results in a shorter time to reach a fixed level of conversion. Raising the pressure from 1 to 5 atmospheres results in a similar reduction in the time required to burn the coal, but further increases in pressure have only a small effect. This is due to the relative importance of the resistance terms in Equation (1). The boundary layer diffusion term is independent of pressure, but the term for combined reaction and pore diffusion is inversely proportional to pressure. Hence the effect of total pressure must be due to non-diffusion controlled regimes for some of the reactions considered, primarily for CO_2 and H_2O.

The required residence time and ash vaporization incurred at a fixed level of conversion are shown in Figure 7 as a function of pressure and equivalence ratio. At a fixed pressure, the residence time is smallest and ash vaporization largest for the fuel-lean case. The effect of raising the pressure is to decrease the amount of ash vaporized, while the required time shows a substantial drop only up to about 5 atmospheres. Another consideration in combustor design is that higher pressures increase the combustion intensity, resulting in lower wall heat losses as a fraction of the thermal coal input and better utilization of the combustor volume.

The tradeoff between ash vaporization and coal combustion efficiency is shown in Figure 8 for stoichiometric combustion. Lower pressures result in more ash vaporization, with the total amount vaporized increasing more rapidly with the fraction of coal burned. Increases in the preheat temperature increases the amount of ash vaporized to a smaller degree.

Two-stage

Calculations were also made under conditions pertinent to two-stage units where the first stage is operated fuel-rich. All of the results presented below were run under adiabatic conditions allowing no heat loss to the combustor walls, and with 15% O_2-enriched air as the oxidant. Figure 9(a) shows the time dependence of coal burnout and gas temperature. Long residence times are required for fuel-rich stoichiometry, and the gas temperature is lower for richer mixtures. In Figure 9(b) changes in pressure are seen to exert similar influences on combustion time and ash vaporization as those for single-stage units. The amount of ash vaporized is not significantly reduced compared to single-stage operation because of the longer residence times and adiabatic conditions.

The contributions to the total rate of carbon oxidation by the different reactive species are shown in Figure 10 as a function of the degree of burnout. The dominant reactions are those with CO_2 and H_2O; the OH contribution is minor and that of O_2 is negligible. This is generally the case when the combustion of volatiles, which is assumed to occur very rapidly prior to char oxidation, consumes all the available oxygen.

The effect of pressure on the time to reach 90% coal burnout (log scale) and on ash vaporization (linear scale) is shown in Figure 11. Raising the pressure lowers both the char oxidation time and the amount of ash vaporized over the entire pressure range. Reducing the equivalence ratio from 2.2 to 1.8 is seen to result in a large decrease in combustion times at the cost of only a slight increase in ash vaporization.

Selection of an optimum residence time for a combustor includes consideration of a number of factors, including the tradeoff with increasing residence time of increases in ash vaporization and carbon burnout. The ash vaporization and selected calculations to show the correlation between the degree of burnout are shown in Figure 12. Increasing the combustor pressure substantially lowers the amount of ash vaporized at a given coal conversion level, but changing the oxidant preheat level results in only a minor change in the amount of vaporization.

It should be noted that the above calculations are for adiabatic operation, a condition which can be approached at the relatively low operating temperatures of a two-stage combustor. If the combustor were not well insulated, the influence of heat losses would be to lower gas and particle temperatures, with consequent reductions in burning rates and ash vaporization. The residence time required to achieve a given burnout level would also be increased, and the overall thermal efficiency of the combustor would be limited either by incomplete fuel utilization or excessive thermal heat losses.

V. Concluding Comments

The above calculations are for an aerodynamically simple combustor and contain a number of approximations concerning the kinetics of devolatilization, char gasification, and ash vaporization. Despite these limitations the model yields reasonable magnitudes for burning times and ash vaporization when compared with the pilot scale studies at BCURA[6]. The value of the model is in providing a measure of the effect of changing operating variables and a means of evaluating different combustion strategies.

Increasing temperature by increasing either the air preheat or lowering the equivalence ratio results in increases in both the amounts of ash vaporized and in the carbon combustion efficiency. For a single-stage combustor the effects of changing equivalence ratio and air preheat are relatively small. For a two-stage combustor, reducing the equivalence ratio results in a pronounced reduction in burning times for relatively modest increases in ash vaporization. Increasing the pressure decreases both the times required to achieve a given burnout and the amounts of ash vaporized. For a single-stage combustor the effect of pressure on ash vaporization is much more significant than on burnout times; for a two-stage combustor the effect of doubling the pressure from 4 to 8 atmospheres results in about a two-fold decrease in burnout times and three-fold decrease in ash vaporization.

From the computations it appears that for a single-stage combustor it would be difficult to achieve high carbon burnout and reduce the ash vaporization to below 18% for combustor conditions of current interest (a pressure of 5 atmospheres and a combustion temperature of 2650°K). For two-stage combustors, operating at equivalence ratios of 1.8 to 2.2, the predicted amount of ash vaporized at 95% carbon burnout again exceeds 15% despite the reduced temperatures. The results of the computation demonstrate the inherent limitations of entrained flow reactors, in which the gas and particle residence times are approximately equal. In order to overcome these constraints it is desirable to have the combustion occur in a cooler regime such as may be encountered at the wall of cyclone reactor where the char particles will reside for periods much greater than the gas residence time. This is, in fact, the strategy currently being pursued in the development of coal combustors for open-cycle MHD. The availability of models for char gasification and ash vaporization should be useful in helping to guide the selection of a combination of equivalence ratio, temperature and reaction time conditions where the dual objectives of high carbon burnout and low ash vaporization may be met.

Acknowledgements

The research reported here forms part of a broader program on the kinetics of coal combustion for MHD applications supported by DOE Contract No. DE-AC01-79ET15518. T. W. Hastings thankfully recognizes fellowship support from the Fannie and John Hertz Foundation.

Nomenclature

A	empirical preexponential factor for vapor pressure
B	empirical heat of vaporization factor for vapor pressure
C	molar concentration
d	diameter
D	diffusion coefficient
f	fraction of total surface area of porous particle
F	fraction of original ash content vaporized
h	convective heat transfer coefficient
$\Delta H_{RX,i}$	enthalpy change per mole of carbon for reaction with gas i
k	intrinsic reaction rate coefficient (sec^{-1})
K	external mass transfer coefficient
N	moles of gas
P	total pressure (atmospheres)
P_i	vapor pressure of ash species i
r	radius
R	universal gas constant
R_i	molar char consumption rate per unit external surface area for reaction with gas i
S_{EX}	external surface area of particle
t	time
T	temperature
V_p	particle volume

Greek Symbols

α_i	moles carbon per mole of reactant i in char oxidation reaction
ϵ	emissivity
ξ	internal effectiveness factor (ratio of reaction rate with pore diffusion to rate without pore diffusion, based on surface concentration)
ϕ	fuel/oxidant equivalence ratio
ϕ_{EFF}	effective coal/air equivalence ratio in gas phase
σ	Stefan-Boltzmann constant

Subscripts

0	initial value
BL	mean value in boundary layer
EX	external surface
g	bulk gas
i	gaseous reactant or ash species
IN	internal surface
P	particle
W	combustor wall

References

1. R. Shuck, T. Hastings, C. Mims, and A.F. Sarofim, "Kinetics of Char Burnout and Ash Vaporization in Coal-Fired MHD Combustors", 18th Symposium on Engineering Aspects of Magnetohydrodynamics, Butte, Montana (1979).

2. J.J. Carberry, Chemical and Catalytic Reaction Engineering, McGraw-Hill, New York (1976).

3. C.N. Satterfield, Mass Transfer in Heterogeneous Catalysis, M.I.T. Press, Cambridge, Mass. (1970).

4. R.B. Bird, W.E. Stewart, and E.N. Lightfoot, Transport Phenomena, John Wiley and Sons, New York (1960).

5. C.A. Mims, M. Neville, R. Quann, and A.F. Sarofim, "Laboratory Studies of Trace Element Transformations During Coal Combustion", Paper presented at the 87th National AIChE Meeting, Boston, Mass., August, 1979.

6. J.B. Heywood and G.J. Womack, Editors, Open Cycle MHD Power Generation, Pergamon Press (1969).

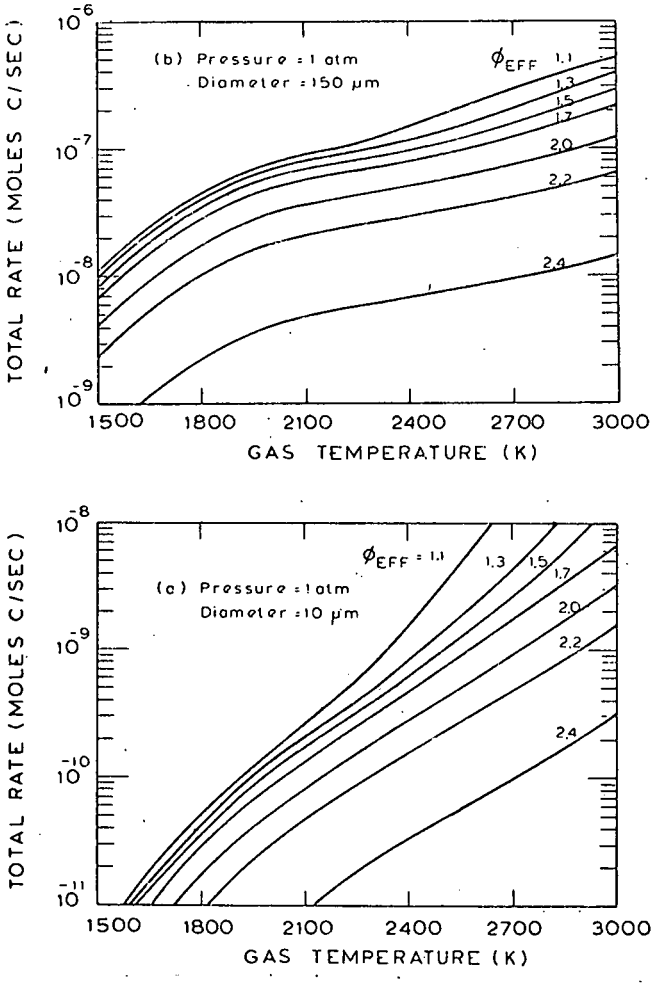

Figure 1. Effects of gas temperature and effective fuel/air equivalence ratio on total char consumption rate for single particle: P = 1 atm; (a) d_p = 10 μm, (b) d_p = 150 μm.

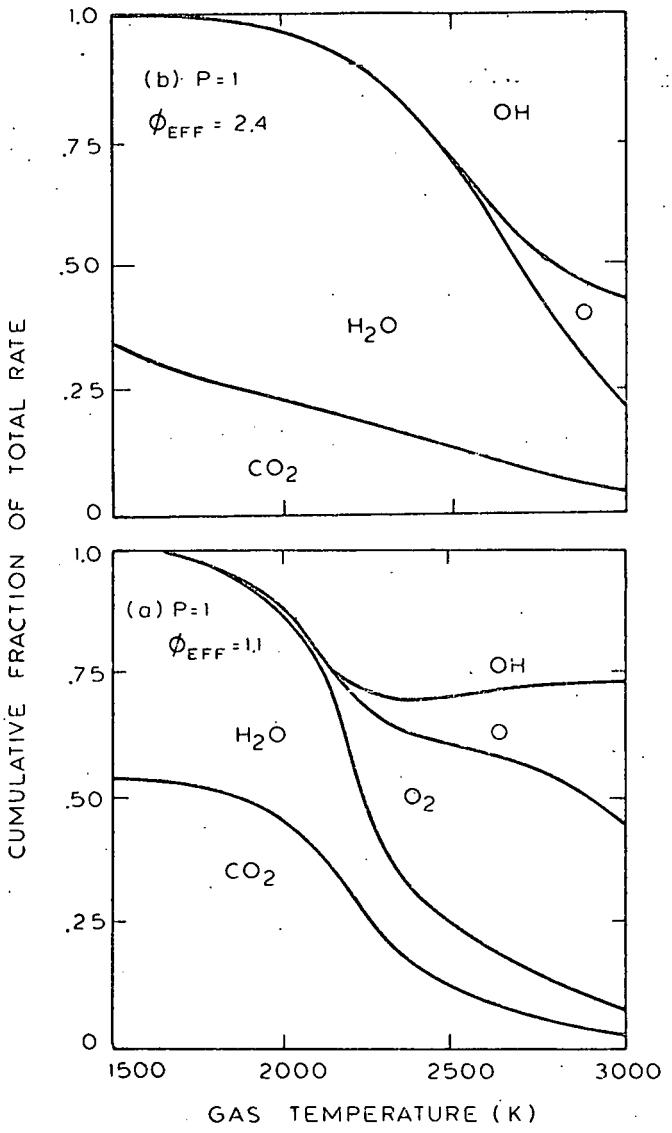

Figure 2. Effect of gas temperature on fraction of total gasification rate contributed by CO_2, H_2O, O_2, O and OH for 10 μm particle: P = 1 atm; (a) ϕ_{EFF} = 1.1, (b) ϕ_{EFF} = 2.4.

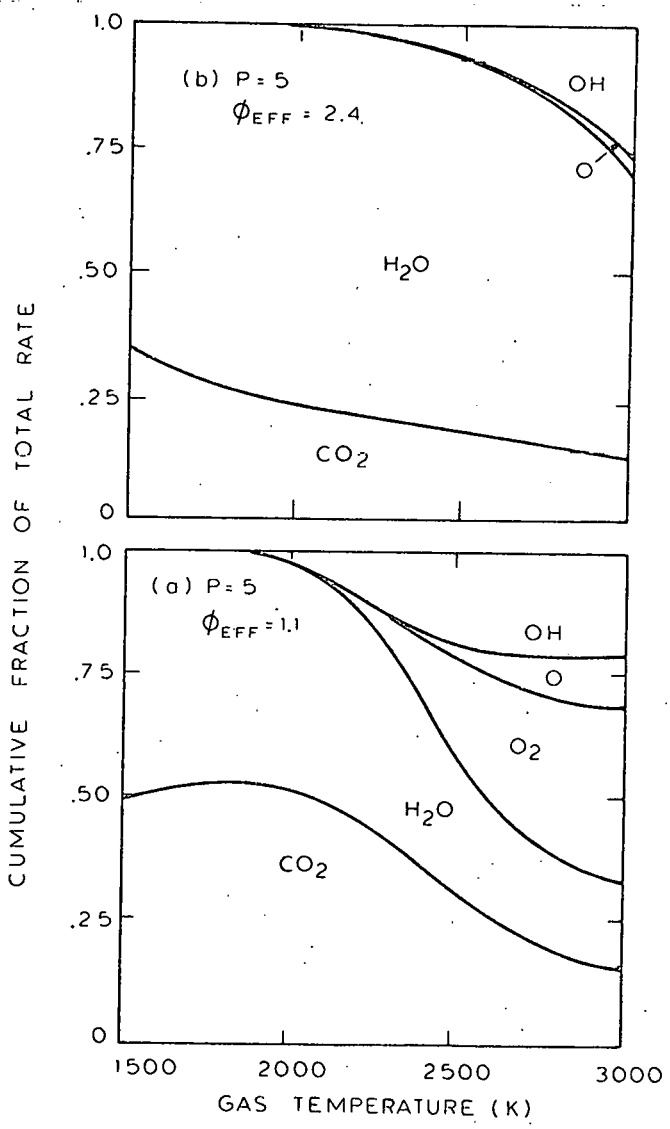

Figure 3. Effect of gas temperature on fraction of total gasification rate contributed by CO_2, H_2O, O_2, O and OH for 10 μm particle: P = 5 atm; (a) ϕ_{EFF} = 1.1, (b) ϕ_{EFF} = 2.4.

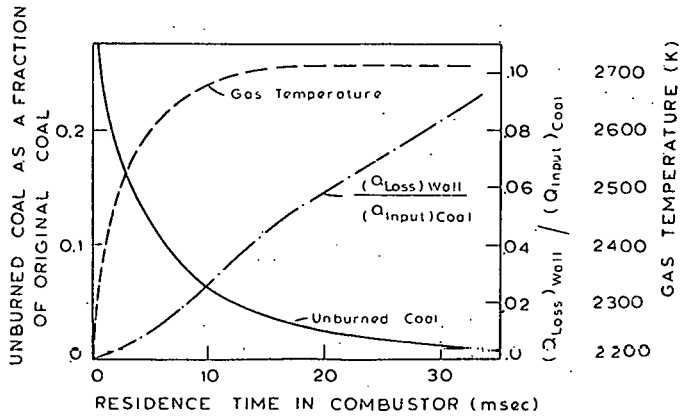

Figure 4. Time dependence of coal burnout, gas temperature, and wall heat loss in a simulated combustor; P = 5 atm, ϕ = 1.0, air preheat temperature = 1600°K. (1 meter square combustor, 70% instant devolatilization, 2.5 kg coal/sec, T_w = 2000°K, Rosin-Rammler size distribution: mean diameter = 31.3 μm, exponent = 1.5).

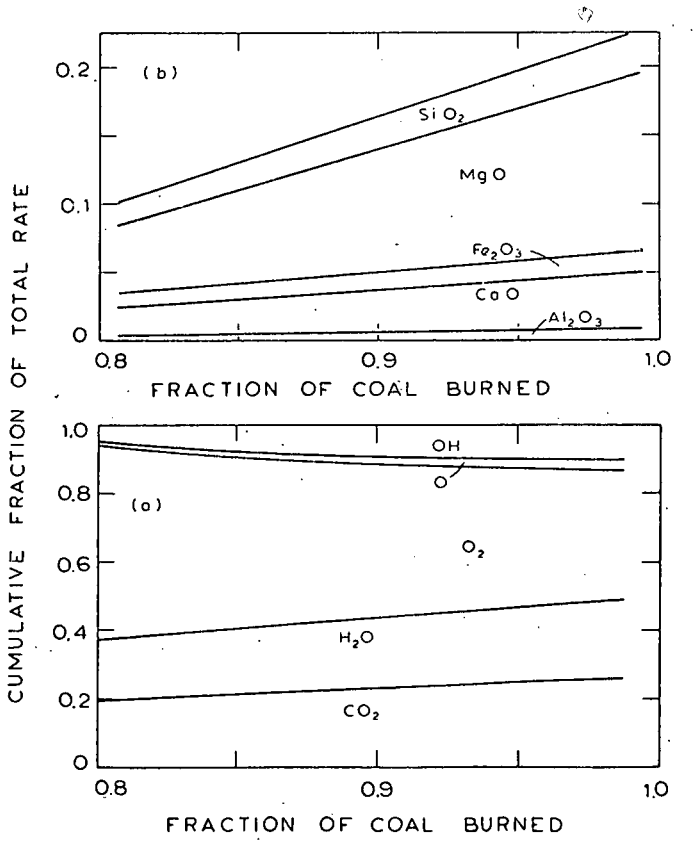

Figure 5. (a) Fraction of total gasification rate contributed by indicated species as a function of coal burnout in a simulated combustor. (b) Contributions to the total ash vaporization by individual mineral constituents as a function of coal burnout. (Conditions are same as those in Fig. 4)

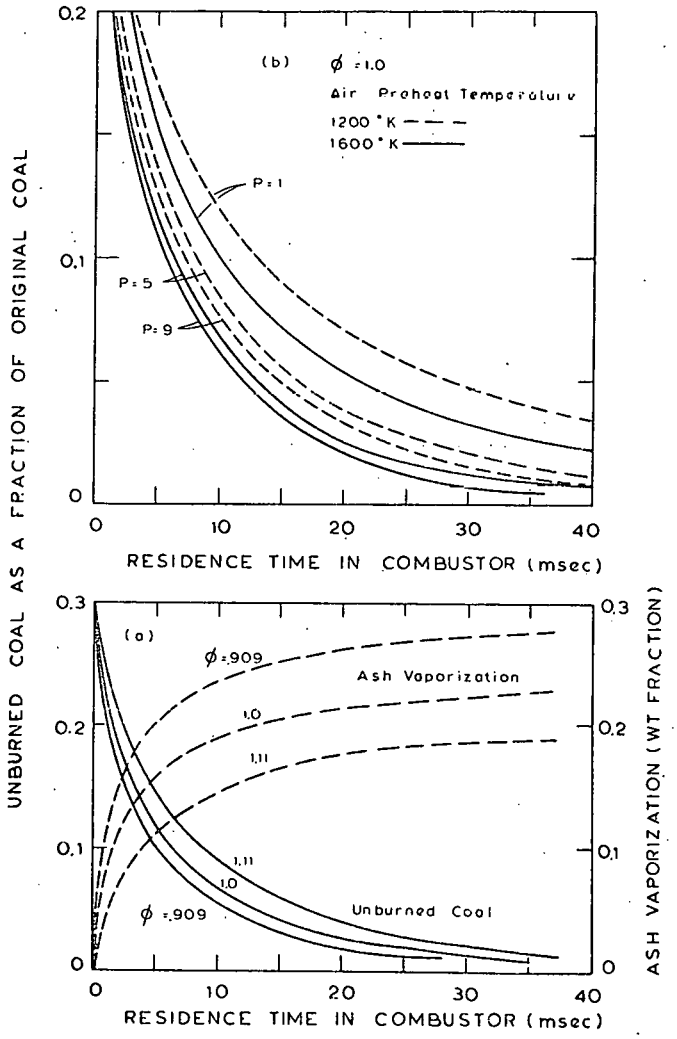

Figure 6. (a) Effects of time and fuel/air equivalence ratio on ocal burnout and ash vaporization in a simulated combustor: P = 5 atm, air preheat temperature = 1600°K.
(b)Effects of time, pressure, and air preheat temperature on coal burnout: ϕ = 1.0.
(Other conditions are same as in Fig. 4)

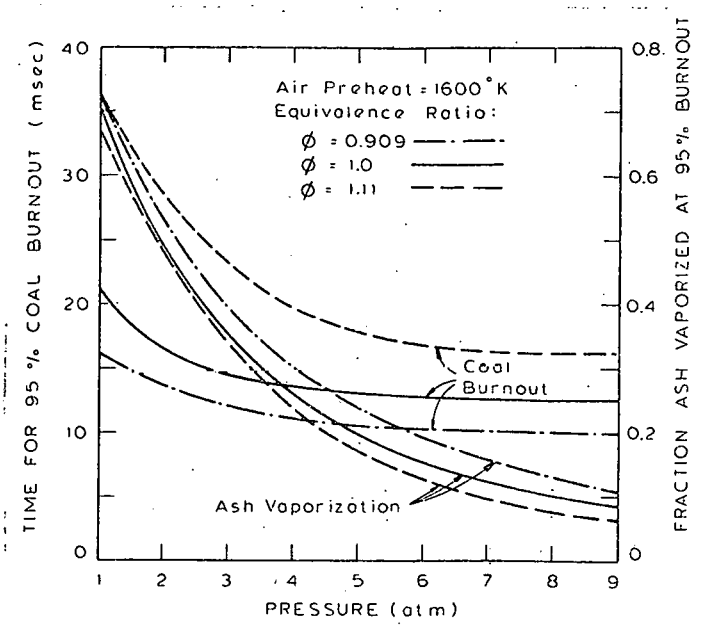

Figure 7. Effects of pressure and fuel/air equivalence ratio on the time and the amount of ash vaporized at 95% coal burnout in a simulated combustor: air preheat temperature = 1600°K. (Other conditions are same as in Fig. 4).

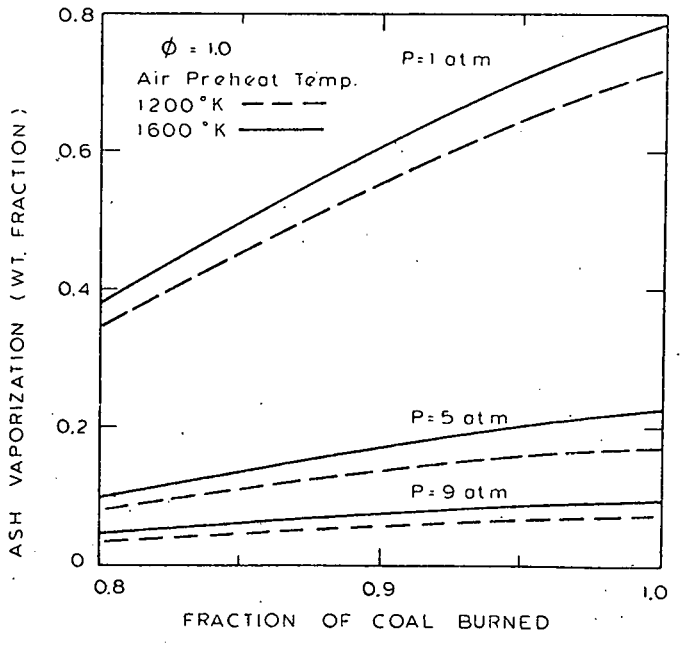

Figure 8. Effects of extent of coal burnout, pressure, and air preheat temperature on the amount of ash vaporized in a simulated combustor: ϕ = 1.0.
(Other conditions are same as in Fig. 4).

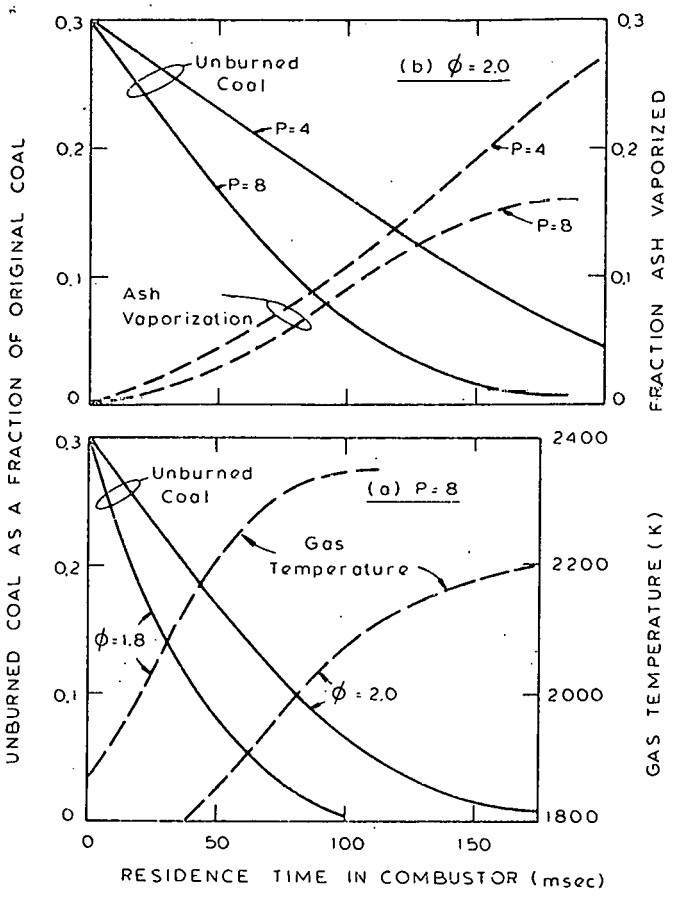

Figure 9. (a) Effects of time and fuel/oxidant equivalence ratio on coal burnout and gas temperature for a simulated adiabatic combustor: oxidant preheat temperature = 1865°K.
(b) Effects of time and pressure on coal burnout and ash vaporization for adiabatic operation: oxidant temperature = 1865°K.
(Oxidant = 15% O_2-enriched air, 1 meter square combustor, 70% instant devolatilization, 2.5 kg coal/sec, T_w = 2000°K, Rosin-Rammler size distribution: mean diameter = 31 μm, exponent = 1.5).

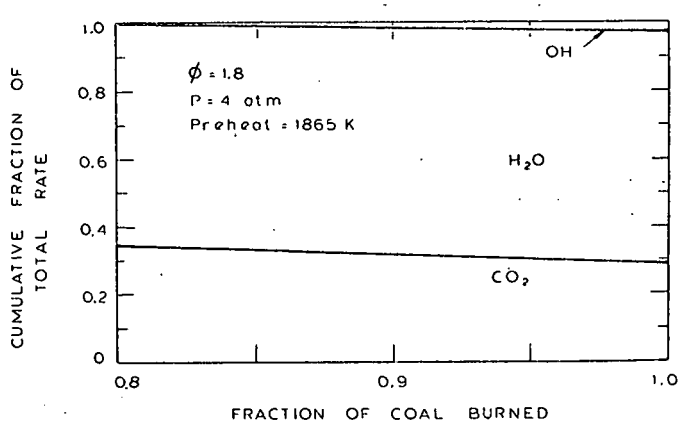

Figure 10. Fraction of total gasification rate contributed by indicated species as a function of coal burnout in a simulated adiabatic combustor: ϕ = 1.8.
(Other conditions are same as in Fig. 9).

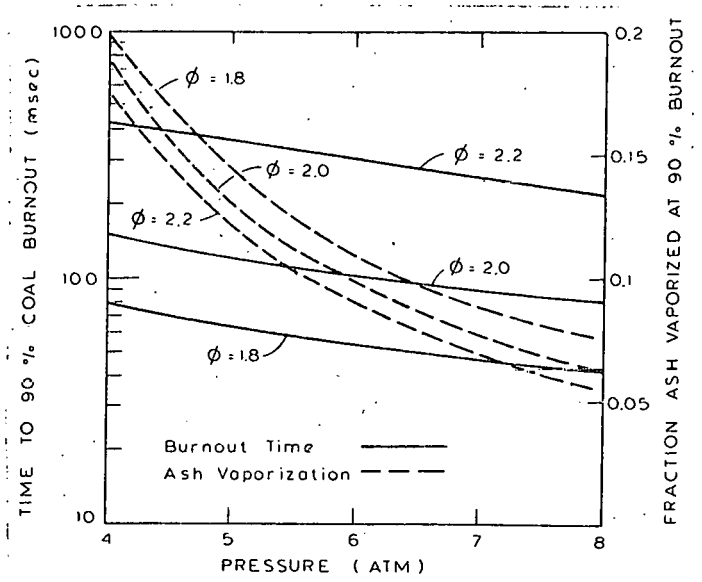

Figure 11. Effects of pressure and fuel/oxidant equivalence ratio on the time and the amount of ash vaporized at 90% coal burnout in a simulated adiabatic combustor: oxidant preheat temperature = 1865°K.
(Other conditions are same as in Fig. 9).

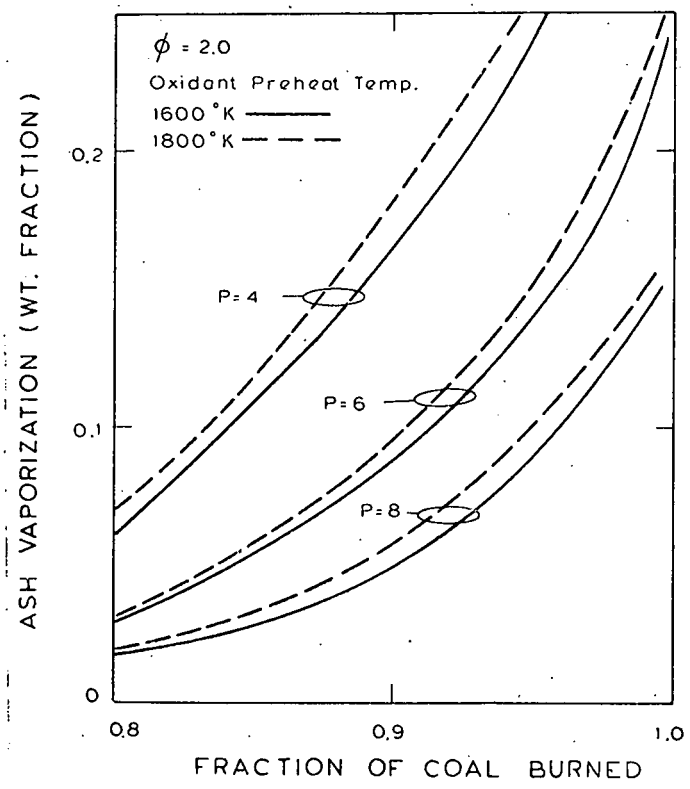

Figure 12. Effects of extent of coal burnout, pressure, and oxidant preheat temperature on the amount of ash vaporized in a simulate adiabatic combustor: oxidant preheat temperature = 1865°K.
(Other conditions are same as in Fig. 9).